American Journal of Environmental Science and Engineering
2020; 4(2): 17-23
http://www.sciencepublishinggroup.com/j/ajese
doi: 10.11648/j.ajese.20200402.12
ISSN: 2578-7985 (Print); ISSN: 2578-7993 (Online)

Assessment and Simulation of Gaseous Dispersion by Computational Fluid Dynamics (CFD): A Case Study of Shiraz Oil Refining Company

Shiva Hashemi[1, *], Dariush Mowla[1, 2], Fereidoun Esmaeilzadeh[1]

[1]School of Chemical and Petroleum Engineering, Shiraz University, Shiraz, Iran

[2]Environmental Research Center in Petroleum and Petrochemical Industries, Shiraz University, Shiraz, Iran

Email address:

Shivahashemi717@gmail.com (S. Hashemi), dmowla@shirazu.ac.ir (D. Mowla), esmaeilzadeh95@gmail.com (F. Esmaeilzade)

[*]Corresponding author

To cite this article:

Shiva Hashemi, Dariush Mowla, Fereidoun Esmaeilzadeh. Assessment and Simulation of Gaseous Dispersion by Computational Fluid Dynamics (CFD): A Case Study of Shiraz Oil Refining Company. *American Journal of Environmental Science and Engineering.* Vol. 4, No. 2, 2020, pp. 17-23. doi: 10.11648/j.ajese.20200402.12

Received: January 13, 2020; **Accepted**: February 24, 2020; **Published**: May 29, 2020

Abstract: Air pollution is simply defined as the presence of any substances such as solids, liquids and gases in the atmosphere, in the adequate amount and time that endangers the life of humans and other living creatures, or damages monuments or properties. In recent years, rapid development of industries including oil and gas industries has led to emit a considerable amount of various gaseous pollutants into the atmosphere. Therefore, developing a reliable model to predict distribution of gaseous pollutants in urban and industrial zones has become an interesting subject among environmental experts. In this study, the distribution of gaseous pollutants emitted from twenty-three stacks of different units located in Shiraz oil refining company is simulated based on the principles of Computational Fluid Dynamics (CFD). To obtain a pattern of pollutants dispersion around the Shiraz refinery, pollutants such as CO, HC, SO_2 and NO are considered. To validate the proposed model, concentration of some pollutants is measured at several points of inside and outside of the refinery area and compared with the corresponding values predicted by the proposed model. Results show that there is a good agreement between the measured data and those obtained from the CFD simulation within 6.3% accuracy. Additionally, the concentrations of SO_2 and HC in outside of refinery are sometimes more than their standard concentrations.

Keywords: Air Pollution, CFD, Gaseous Pollutants Dispersion, Shiraz Oil Refining Company

1. Introduction

Recently, development of industries with the growth of population leads to the investigation of environmental pollutants transportation and distribution that has become a major concern especially in urban areas. Air pollution is happened by introducing substances such as gaseous, liquids or solids into the Earth's atmosphere that may cause harm to human life, other living organisms and also may damage the natural or built environment. So, knowing the concentration of different pollutants in the ambient of an industrial zone is indispensable for minimizing their damages [1].

Beside, air sampling and analysis are costly and time-consuming and not reliable due to their dependence on ambient and operational conditions. Data obtained for one day at a given location may not be valid for the next day at the same location [2].

Among various dispersion models, the Gaussian plume model is the most well-known analytic model for predicting the distribution of air pollutants. It is computationally much more affordable, compared with other models in terms of time and modeling efforts particularly in large scale studies [3]. By contrast, the concentration is related to the wind speed causing to overestimation of concentration when the wind speed is less than 2 m/s or close to zero [4]. Some researchers reported that the steady state Gaussian plume model (GPM) generally overestimates the ground level concentration of gaseous pollutants in low wind conditions [5].

Moreover, with a dramatic improvement in computer

hardware capacity and numerical algorithms, the CFD models have become one of the common tools to simulate and predict gaseous pollutants distribution in real areas [6-8].

In addition, the ability to expect ground level concentration of air pollutants is necessary to define the environmental impact of existing sources to estimate alternative new source locations, designs, controls and to estimate the effect of possible modifications to existing sources [9]. Computational Fluid Dynamics (CFD) is a numerical calculation technique for extracting current flow information, fluid properties and other phenomena associated with flow such as heat transfer, mass transfer and reactions in different systems [10]. Although a lot of input data and much time are required, the numerical method using CFD simulation is a beneficial tool in air quality assessment. Such models can define the distribution of gaseous pollutants if they are properly set up, and boundary conditions are correctly applied [3].

Many researchers have studied the performance of CFD model in predicting pollutants concentrations in urban and industrial zones. Tominaga and Stathopoulos carried out CFD modeling involving Reynolds-Averaged Navier-Stokes (RANS) equation and large eddy simulation (LES) model to predict the distribute of gaseous pollutants related to a street canyon [11]. Rahimi, Tavakoli and Zahiri applied CFD model to predict gaseous pollutants dispersion emitted from various stacks in refinery of Esfahan [12].

Some investigations have also been evaluated in geometrically complex situations including few obstacles [13, 14].

Some previous studies were examined by Koeltzsh and realized that Sc_t is one of the important factors (in the range of 0.5 to 0.9) with considerable effects on gaseous pollutant distribution [15].

In this work, a CFD model is performed to obtain the dispersion of gaseous pollutants (CO, HC, SO_2 and NO) emitting from 23 different stacks of Shiraz oil refining company. In addition, the effect of different parameters including wind velocity, ambient temperature and surface roughness upon gaseous dispersion is elucidated.

2. Methodology

2.1. Description of the Studied Area

Shiraz oil refining company was established in 1973 and located in the north east of Shiraz city, Iran. The refinery actually is composed of atmospheric and vacuum crude distillation unit, visbreaker, isomax unit, catalyst reforming, naphta unifying unit, hydrogen, merox, amin treating unit, waste water stripping section and sulphur recovery plant (SRU). Residential area to the north east of refinery is within 8,000 m from the refinery boundary and could be at risk due to 23 stacks emissions. The studied area is shown in Figure 1, a cartesian coordinate X, Y and Z was used, being X horizontal and parallel to the wind direction, Y perpendicular to the wind direction and Z, vertical. The domain dimensions that are 12 Km × 5 Km × 0.3 Km are applied to estimate the gaseous dispersion of pollutants such as CO, NO, SO_2 and HC inside the assessed area using CFD simulation. To validate the proposed model, the CO and SO_2 concentrations are also measured inside and outside of the refinery boundaries predict the concentration of pollutants around the refinery area.

The governing equations are:

$$\frac{\partial \rho}{\partial t} + \nabla \cdot (\rho \vec{v}) = 0 \quad (1)$$

$$\frac{\partial}{\partial t}(\rho \vec{v}) + \nabla \cdot (\rho \vec{v} \vec{v}) = -\nabla \mathrm{p} + \nabla \cdot (\bar{\tau}) + \rho \vec{g} \quad (2)$$

$$\frac{\partial (\rho C_v T)}{\partial t} + \nabla \cdot (\rho \vec{v} C_P) = \nabla \cdot (k_T \nabla T) \quad (3)$$

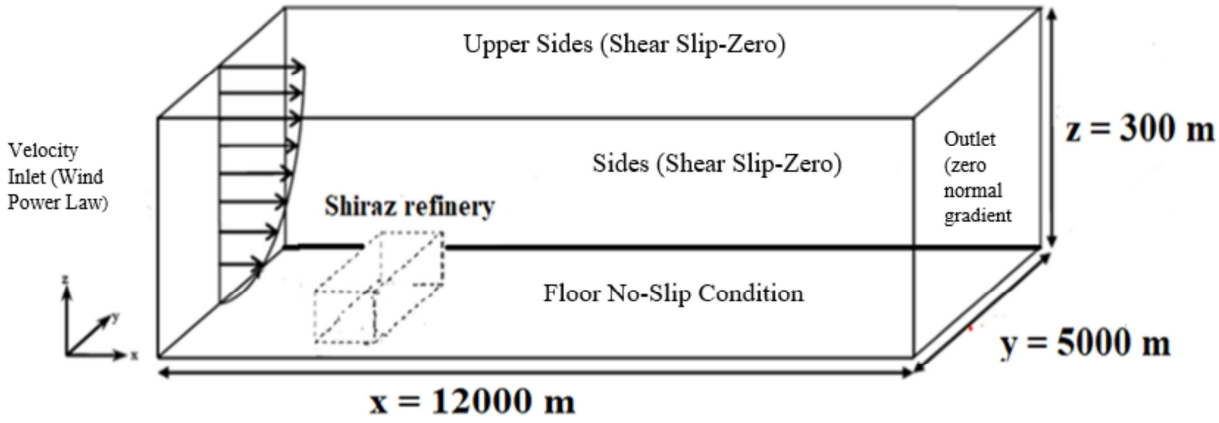

Figure 1. *Shematic diagram of the studied region around the shiraz refinery.*

To generate grid, the Gambit software was used. Regarding the number of cells and time-consuming, some modifications are made to limit the number of cells and make the model more efficient. So, the unstructured grid or mesh system was used to divide the computational domain into 1,952,443 cells.

2.2. Measured Data

The measurements are performed using a Testo-350

analyzer to measure the concentration of CO, NO, SO_2 and HC from twenty-three different stacks from June 2016 to June 2018. The stack's diameter, height, exit temperature, gas exit velocity and mole fraction of the pollutants are given in Table 1.

Additionally, SO_2 and CO concentrations are measured at four locations of inside and outside of the refinery boundary using an Aeroequal analyzer presented in Tables 2 and 3. The mean values for wind speed, direction and ambient temperature are 1.2 m/s, W-SW and 16 ˚C, respectively.

Table 1. *Stacks characteristics of point sources.*

NO.	d	h	T	v	X_{CO}	X_{NO}	X_{SO2}	X_{HC}
	m	m	k	m/s	ppm	ppm	ppm	ppm
Boil. A	1.524	29.5	668	7.9	16.5	54.0	11.5	902.0
Boil. B	1.524	29.5	486	8.1	8.5	67.8	1.0	660.0
Boil. C	1.524	29.5	543	8.9	13	60.0	0.0	563.0
Boil. D	1.524	29.5	554	9.5	8.0	44.0	0.0	616.0
Boil. E	1.524	29.5	599	10.2	18.0	62.5	1.0	706.3
Boil. F	1.524	29.5	534	8.5	8	64.6	0.0	517.7
101 A	2.26	48	701	8.3	10.0	62.0	1.0	199.0
101 B	1.75	36	706	8.7	7.0	60.0	0.6	261.0
102	1.55	48	587	9.1	8.7	58.6	0.5	427.0
201	0.9	32	636	6.5	11.5	54.0	3.0	229.0
202	0.7	32	746	6.5	12.0	57.0	3.0	265.0
203	2.6	32	601	6.0	13.0	48.0	6.0	173.0
206	0.9	32	568	7.0	13.0	59.8	1.0	122.0
301	1.8	31	551	7.0	12.4	53.2	0.0	353
401	0.75	32	609	7.0	32.6	61.6	0.8	134.0
402	0.75	32	603	7.0	23.4	42.7	0.0	260.0
601	2.64	36	674	7.0	24.5	40.0	0.0	419.0
602	1.92	36	643	7.0	11.7	50.0	0.0	278.0
603	1.1	36	616	7.0	30.0	53.6	0.0	245.0
701 A	1.62	59.6	517	6.0	6.0	67.8	1.0	340.0
701 B	1.62	59.6	517	5.2	3.8	69.5	1.0	377.0
901	1	30	787	6.5	612.0	60.0	1167.0	5071.0
Inc	1.07	30	998	7.0	80.0	38.5	2843.0	203.0

3. Mathematical modeling

3.1. Governing Equations

The widespread technique applied to solve the Navier-Stokes (NS) equations is the time averaged, in which the equations are changed into the Reynolds Averaged Navier-Stokes (RANS) set [16]. The conservation laws of mass, energy and momentum are applied to

where ρ is the density, v the velocity, t the time, τ the shear stress, p the pressure, g the gravity acceleration, T the temperature, C_v and C_P the specific heats and k_T the thermal conductivity. In this study, the $k-\varepsilon$ standard model is used to represent the effects of turbulence. This model introduces two additional transport equations for turbulent kinetic energy, k, (Eq. 4) and turbulent kinetic energy dissipation rate ε, (Eq. 5), respectively [17]:

$$\frac{\partial}{\partial t}(\rho k)+\frac{\partial}{\partial x_i}(\rho k u_i)=\frac{\partial}{\partial x_j}[\left(\mu+\frac{\mu_T}{\sigma k}\right)\frac{\partial k}{\partial x_j}+G_k+G_b-\rho\varepsilon-Y_M \tag{4}$$

$$\frac{\partial}{\partial t}(\rho \varepsilon)+\frac{\partial}{\partial x_i}(\rho \varepsilon u_i)=\frac{\partial}{\partial x_j}[\left(\mu+\frac{\mu_T}{\sigma \varepsilon}\right)\frac{\partial \varepsilon}{\partial x_j}+C_{\varepsilon 1}\frac{\varepsilon}{k}\left(G_k+C_{\varepsilon 3}G_b\right)-C_{\varepsilon 2}\rho\frac{\varepsilon^2}{k}+S_\varepsilon(z) \tag{5}$$

where u_i is the velocity component along x_i direction, μ the viscosity, μ_T the turbulent viscosity, G_k the shear stress-related turbulent kinetic energy production, G_b the buoyance-related turbulent kinetic energy production and Y_M the compressibility-related kinetic energy production.

3.2. Boundary Conditions

The considered domain and its boundary conditions are shown in Figure 1. The wind speed is one of the most important parameters in the pollutants dispersion, since the corresponding boundary condition should take into account the frictional effects near the ground level. The inflow wind speed was adjusted to obey power law correlation as shown in (Eq. 6).

$$u_z=u_0\times\left(\frac{Z}{Z_0}\right)^n \tag{6}$$

where n is a dimensionless parameter, relying on atmospheric stability conditions and surface roughness. The exit face of the stack was defined as a velocity inlet with uniform velocity profile. Turbulence quantities are calculated based on the hydraulic diameter and turbulence intensity was considered to be 10% [18]. The bottom of domain was defined by no-slip conditions. The both top and sides of the domain, symmetry boundary conditions are prescribed. At the outlet, the zero static pressure was imposed [19].

Subsequently, the Navier-Stokes equations were solved using Fluent software. The k-ε standard model was applied to provide closure. The steady-state analysis was performed, and the second order upwind scheme was utilized to discretize. Because, that scheme was particularly adapted for unstructured grids [20]. The SIMPLE algorithm was chosen for the calculations of velocity and pressure. The convergence criterion was set to residuals equal or less than 10^{-4} for the continuity equation.

3.3. Statistical Parameters

To evaluate the performance of the earlier mentioned turbulent models, the statistical evaluation parameters reported by Hanna [21] and summarized by Chang and Hanna [22] as follows:

$$FB = 2\frac{(\overline{C_0}-\overline{C_P})}{(\overline{C_0}+\overline{C_P})} \quad (7)$$

$$MG = exp(\overline{ln\, C_0} - \overline{ln\, C_P}) \quad (8)$$

$$NMSE = \frac{\overline{(C_0-C_p)^2}}{\overline{C_P}\,\overline{C_0}} \quad (9)$$

$$VG = \exp\left[\overline{(lnC_0 - lnC_p)^2}\right] \quad (10)$$

where FB, MG, $NMSE$, VG, C_0 and C_p denote the fractional bias, geometric mean bias, normalized mean square error, geometric variance, observed concentrations, and the predicted concentrations, respectively.

The typical values for an acceptable model performance including FB, MG, NMSE and VG were reported by Milliez and Carissimo [22, 23], respectively, $-0.3 < FB < 0.3$, $0.7 < MG < 1.3$, $NMSE < 4$ and $VG < 1.6$.

4. Results and Discussion

4.1. Choose the Best Turbulence Schmidt Numbers

Five turbulence Schmidt numbers were evaluated using statistical parameters to choose the best result related to SO_2 (Table 2). According to this table, Sct=0.4 gives the better result than the other values of Sct.

Table 2. *The statistical parameters (SP) for Gaussian Plume Model (GPM) and k-ε standard model with different Sct values.*

SP	Ideal value	Standard k-ε					GPM
		Sct=0.3	Sct=0.4	Sct=0.5	Sct=0.6	Sct=0.7	
FB	0	0.076	0.014	0.082	0.095	0.087	-0.105
NMSE	least	0.042	0.015	0.100	0.210	0.300	0.760
MG	1	1.030	1.050	1.100	1.220	1.360	1.400
VG	1	1.040	1.004	1.200	1.390	1.740	1.800

4.2. Validation

Tables 3 and 4 show the results of field measurements against those obtained from the CFD simulation for SO_2 and CO pollutants, respectively.

According to Table 3, there is a good agreement between results of the proposed model and experimental data.

Table 3. *Measurement results against the CFD simulation for SO_2 pollutant.*

NO.	Sampling location		SO_2 (ppm)	
	Latitude	Longitude	EXP	CFD
1	29°44'19.3"	52°39'28.8"	0.030	0.027
2	29°44'23.6"	52°39'55.6"	0.070	0.069
3	29°44'58.9"	52°41'9.223"	0.040	0.038
4	29°45'46.8"	52°41'595.9"	0.000	0.008

Table 4. *Measurement results against the CFD simulation for CO pollutant.*

NO.	Sampling location		CO (ppm)	
	Latitude	Longitude	EXP	CFD
1	29°44'19.3"	52°39'28.8"	0.000	0.100
2	29°44'23.6"	52°39'55.6"	1.910	0.280
3	29°44'58.9"	52°41'9.223"	2.180	0.160
4	29°45'46.8"	52°41'595.9"	3.500	0.080

As shown in Table 4, there is a considerable difference between the measured and calculated values for CO concentration at different locations.

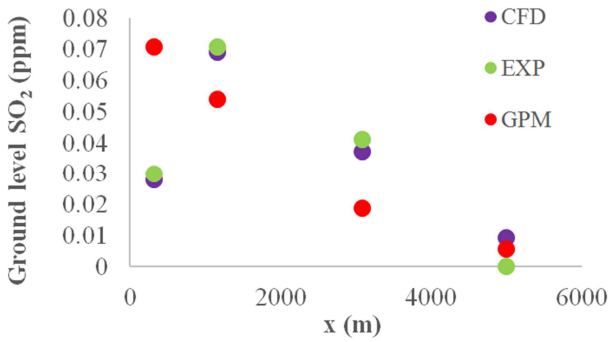

Figure 2. *Comparison results of the measured data with those obtained from the CFD model and GPM.*

This difference can be attributed to the emission of CO from other sources than Shiraz oil refinery such as Shiraz-Isfahan highway and adjacent industries like industrial Abarik region. Furthermore, the results of the proposed model are also compared with those obtained from Gaussian Plume model that is shown in Figure 2 As can be seen, the results of the CFD model are much closer to the measured values. Additionally, as shown in Figure 2, the average error of SO_2 concentrations obtained from the proposed model is about 6.3% in comparison with the measured values.

4.3. Gaseous Pollutants Distribution

The effect of different input parameters of the CFD model on the ground level concentration profile is presented in Figures 3-7.

The emission of NO ground level concentration at different wind speeds including 3, 5 and 8 m/s is shown in Figure 3. As can be seen, the maximum concentration of NO pollutant occurs at a distance far away from the pollutant source with increasing the wind speed. Likewise, the maximum concentration of NO pollutant at higher wind speeds is less than that at lower wind speeds. Consequently, since the mixing of pollutants occurs better at higher wind speeds; hence, the maximum ground level concentration of the pollutant declined.

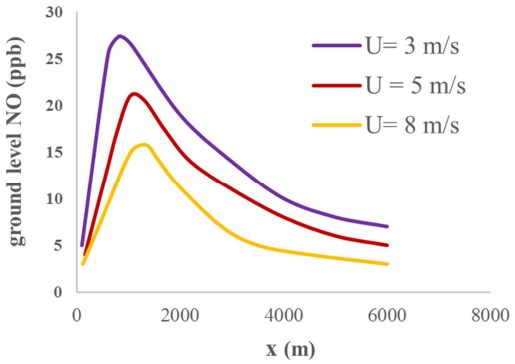

Figure 3. *Emission of NO concentration at different wind speeds.*

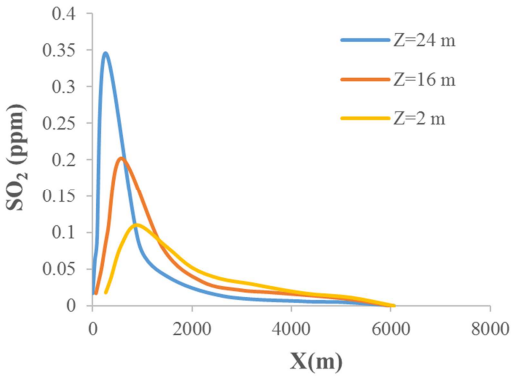

Figure 4. *Distribution of SO_2 concentrations at altitudes of 2, 16 and 24 meters from the ground level.*

According to Figure 4, the comparison of SO_2 concentrations at different altitudes shows that at a height of 24 meters above ground level, the maximum SO_2 concentration occurs at a distance of about 260 meters away from the stack-901. Also at altitudes of 16 and 2 meter from the ground surface, the maximum concentration happens at the distance of about 580 and 800 meters away from the stack-901, respectively. Therefore, one can conclude that at higher altitudes, the maximum concentration of SO_2 occurs near the stack. Additionally, the maximum concentration at higher altitudes is higher than that at lower altitudes.

The effect of surface roughness on CO emission is shown in Figure 5. By increasing the surface roughness, the distribution range of the CO concentration reduces, and the maximum concentration on the ground level decreases and occurs at a closer distance from the pollutant source.

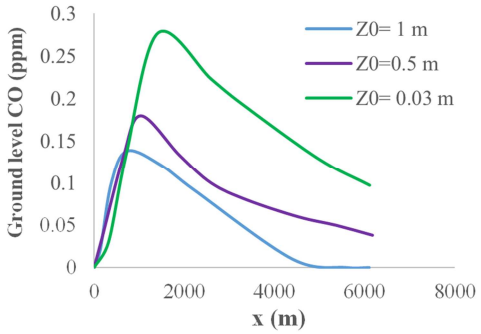

Figure 5. *The effect of surface roughness on CO distribution.*

Figure 6 shows that how the NO pollutant distributes along y (perpendicular to the direction of the dominant wind) at different distances. With a distance of about 100, 300 and 600 meters away from the stack-201 in the dominant wind direction (x), the maximum ground level concentrations of NO are 19, 32 and 36 ppb, respectively. In other words, it can be stated that, up to a distance of about 600 meters away from the stack-201, not only the NO distribution increases in the y direction, but also the values of NO concentration increase at ground level. However, at distances of 2000 and 5000 meters away from the stack-201, the maximum NO concentration reduces because of the spread of pollutants by wind causing the width of NO ground level concentration to widen far beyond the stack-201.

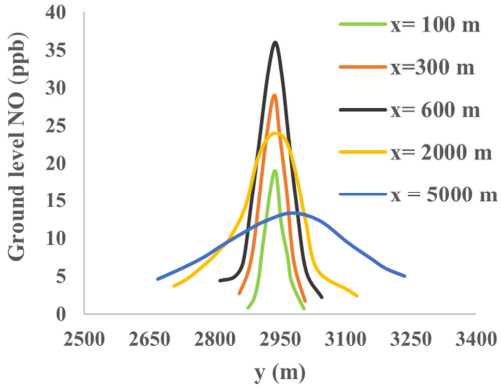

Figure 6. *Distribution of NO concentration along y-direction at different distances.*

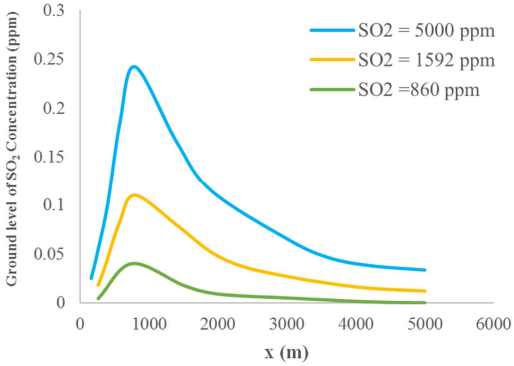

Figure 7. *The distribution of SO_2 concentration with the emission concentration of 5000, 1592 and 815 ppm from the stack-901.*

The distribution of SO_2 concentration with the emission concentration of 5000, 1592 and 815 ppm from the stack-901 is shown in Figure 7. According to this figure, as expected, the ground level concentration of SO_2 reduces with the reduction of SO_2 emission concentration from the stack.

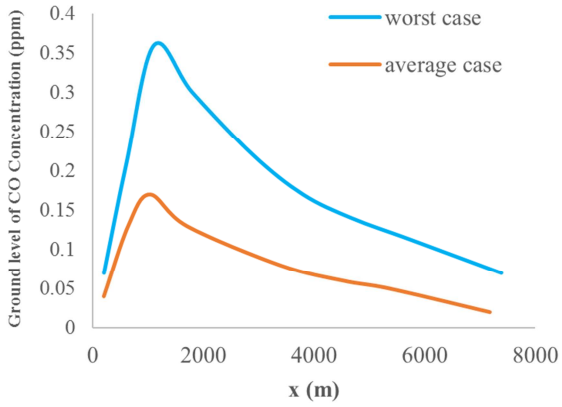

Figure 8. *CO pollutant distribution.*

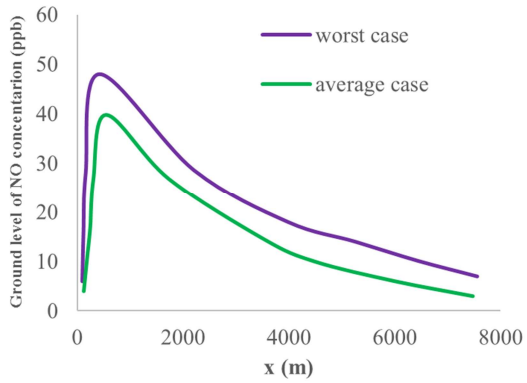

Figure 9. *NO pollutant distribution.*

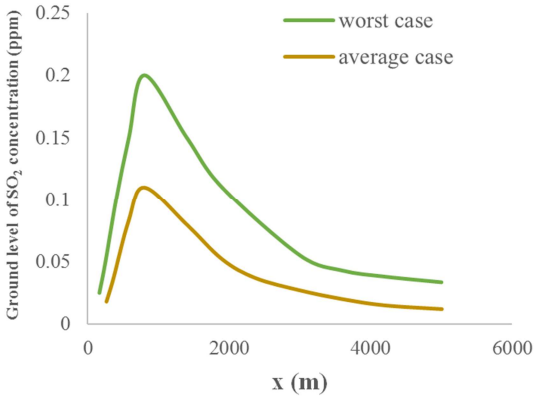

Figure 10. *SO_2 pollutant distribution.*

The dispersion of pollutants such as CO, NO, SO_2 and HC in annual average conditions (average exhaust concentration from the stack; CO=612 ppm, NO=60 ppm, SO_2=1167 ppm and HC=507 ppm, average ambient temperature=16°C and average wind velocity=1.2 m/s) and the worst conditions (the highest exhaust concentration; CO=1543 ppm, NO=77 ppm, SO_2=5000 ppm and HC=960 ppm emitted from the stack, minimum ambient temperature=-1.4°C and stagnant) are shown in the Figures 8-11. The predicted values of HC and SO_2 concentrations in the worst conditions are higher than those in ambient standard concentrations, while for annual average conditions, only SO_2 concentration is higher than that ambient standard concentration. The WHO (World Health Organization) standards for CO, NO, SO_2 and HC are 9 ppm, 53 ppb, 0.037 ppm and 0.24 ppm, respectively.

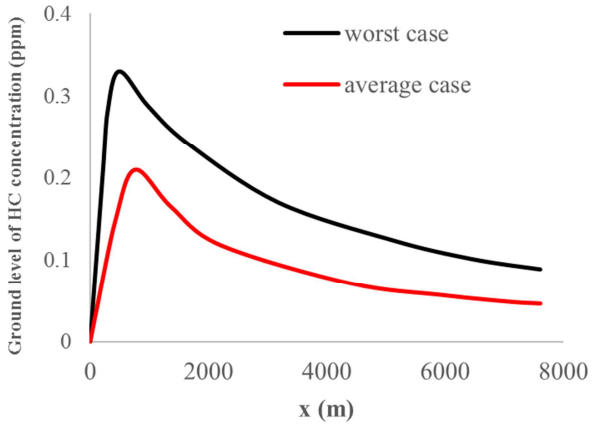

Figure 11. *HC pollutant distribution.*

5. Conclusions

In this study, CFD simulation was introduced as a new approach for the prediction of gaseous pollutants distribution, including CO, NO, SO_2 and HC from Shiraz oil refining company. The k–ε standard model is investigated to simulate the turbulent flow field. The impact of turbulence Schmidt number (Sct), wind velocity, surface roughness and different exhaust concentrations from 23 stacks on pollutants distribution was considered. The minimum error is gained for standard k–ε turbulent model using statistical parameters. The standard k–ε model with Sct=0.4 treat as the best values. The CO and SO_2 concentrations are also measured inside and outside of the refinery boundaries which are compared with the experimental measurements. At last, other results of the simulation presented that:

Although the concentration of all gaseous pollutants from the refinery in the city of Zarghan is lower than the ambient standard concentration, in the worst condition, only the concentration of SO_2 pollutant in some part of adjacent industries like industrial Abarik region is higher than those in ambient standard concentrations. In the annual average conditions, with a reduction of approximately 50% in the exhausting SO_2 concentration from the stack 901, the maximum SO_2 concentration at ground level is lower than the ambient standard concentration.

Acknowledgements

The authors would like to thank the Environmental Research Centre in Petroleum and Petrochemical Industries of Shiraz University and also Shiraz Oil Refinery Company, Shiraz, Iran for their technical supports.

References

[1] Odigure J. O., "Safety Loss and Pollution Control in Chemical Process Industries," pp. 80–93, 1998.

[2] Perry R. H., *Chemical Engineers Hand Book*, 7th ed. USA: Mc - Graw Hill International USA, 1984.

[3] M. Bady, "Evaluation of Gaussian Plume Model against CFD Simulations through the Estimation of CO and NO Concentrations in an Urban Area," *Am. J. Environ. Sci.*, vol. 13, pp. 93–102, 2017.

[4] P. Goyal and T. V. B. P. S. Rama Krishna, "Dispersion of pollutants in convective low wind: A case study of Delhi," *Atmos. Environ.*, vol. 36, no. 12, pp. 2071–2079, 2002.

[5] A. Namdeo, G. Mitchell, and R. Dixon, "TEMMS: an Integrated Package for Modelling and Mapping Urban Traffic Emissions and Air Quality," *Environ. Model. Softw.*, vol. 17, no. 2, pp. 177–188, 2009.

[6] S. M. Tauseef, D. Rashtchian, and S. A. Abbasi, "CFD-based simulation of dense gas dispersion in presence of obstacles," *J. Loss Prev. Process Ind.*, vol. 24, no. 4, pp. 371–376, 2011.

[7] B. R. Cormier, R. Qi, G. W. Yun, Y. Zhang, and M. Sam Mannan, "Application of computational fluid dynamics for LNG vapor dispersion modeling: A study of key parameters," *J. Loss Prev. Process Ind.*, vol. 22, no. 3, pp. 332–352, 2009.

[8] S. Sklavounos and F. Rigas, "Simulation of Coyote series trials—Part I:," *Chem. Eng. Sci.*, vol. 61, no. 5, pp. 1434–1443, 2005.

[9] S. Baroutian, A. Mohebbi, and A. S. Goharrizi, "Measuring and modeling particulate dispersion : A case study of Kerman Cement Plant," *J. Hazard. Mater.*, vol. 136, pp. 468–474, 2006.

[10] X. Xie, Z. Huang, and J. S. Wang, "Impact of building configuration on air quality in street canyon," *Atmos. Environ.*, vol. 39, no. 25, pp. 4519–4530, 2005.

[11] Y. Tominaga and T. Stathopoulos, "CFD modeling of pollution dispersion in a street canyon: Comparison between LES and RANS," *J. Wind Eng. Ind. Aerodyn.*, vol. 99, no. 4, pp. 340–348, 2011.

[12] P. Taylor, A. Rahimi, T. Tavakoli, and S. Zahiri, "Computational Fluid Dynamics (CFD) Modeling of Gaseous Pollutants Dispersion in Low Wind Speed Condition: Isfahan Refinery, a Case Study," *Pet. Sci. Technol.*, no. 32, pp. 1318–1326, 2014.

[13] H. A. Olvera, A. R. Choudhuri, and W. W. Li, "Effects of plume buoyancy and momentum on the near-wake flow structure and dispersion behind an idealized building," *J. Wind Eng. Ind. Aerodyn.*, vol. 96, no. 2, pp. 209–228, 2008.

[14] P. Neofytou, A. G. Venetsanos, D. Vlachogiannis, J. G. Bartzis, and A. Scaperdas, "CFD simulations of the wind environment around an airport terminal building," *Environ. Model. Softw.*, vol. 21, no. 4, pp. 520–524, 2006.

[15] KonradKoeltzsch, "The height dependence of the turbulent Schmidt number within the boundary layer," *Atmos. Environ.*, vol. 34, no. 7, pp. 1147–1151, 2000.

[16] A. Luketa-Hanlin, R. P. Koopman, and D. L. Ermak, "On the application of computational fluid dynamics codes for liquefied natural gas dispersion," *J. Hazard. Mater.*, vol. 140, no. 3, pp. 504–517, 2007.

[17] D. Parrish, S. T. Schneider, J. Healey, K. Lunde, J. O. Conner, and S. Compton, "Fluent 6 User's Guide," 2002.

[18] M. Bady, S. Kato, and H. Huang, "Towards the application of indoor ventilation efficiency indices to evaluate the air quality of urban areas," *Build. Environ.*, vol. 43, no. 12, pp. 1991–2004, 2008.

[19] M. Pontiggia and D. Appolonia, "CFD model simulation of LPG dispersion in urban areas," *J. Hazard. Mater.*, vol. 176, pp. 589–596, 2010.

[20] H. Huang, R. Ooka, and S. Kato, "Urban thermal environment measurements and numerical simulation for an actual complex urban area covering a large district heating and cooling system in summer," *Atmos. Environ.*, vol. 39, no. 34, pp. 6362–6375, 2005.

[21] S. R. Hanna, J. C. Chang, and D. G. Strimaitis, "HAZARDOUS GAS M O D E L EVALUATION WITH," *Atmos. Environ.*, vol. 27, no. 15, pp. 2265–2285, 1993.

[22] J. C. Chang and S. R. Hanna, "Air quality model performance evaluation," *Meteorol. Atmos. Phys.*, vol. 87, no. 1–3, pp. 167–196, 2004.

[23] M. Milliez and B. Carissimo, "Numerical simulations of pollutant dispersion in an idealized urban area, for different meteorological conditions," *Boundary-Layer Meteorol.*, vol. 122, no. 2, pp. 321–342, 2007.